PARTEC 2004

# Powder flow behavior for cohesive frictional materials

**Stefan Luding**[1,2]

[1] Particle Technology, DelftChemTech, TU Delft, Julianalaan 136, 2628 BL Delft, The Netherlands

[2] e-mail: s.luding@tnw.tudelft.nl

## ABSTRACT

Powder flow behavior can be measured by experiments on a Jenike cell, a ring shear tester, or a bi-axial box. We choose the latter boundary condition for our discrete element simulations and examine the effect of friction and other "microscopic" forces. From the discrete particle simulation, macroscopic field variables like stress can be obtained from averaged micro-quantities on the contact- level. The outcome of such a coarse-grained homogenization procedure can be compared to the macroscopic observations on the boundaries of the system, and the macroscopic parameters, as obtained here from the simulations, can be used for the constitutive modeling of the powder flow behavior.

## 1 INTRODUCTION

The flow behavior of powders under large deformations is studied, using the discrete element method (DEM), a convenient tool to gain insight into the evolution of, e.g., shear localization. Powders are typically inhomogeneous, non-linear, disordered, and an-isotropic on a “microscopic” scale [1-3], where the typical microscopic size is the particle size. An irregular, random packing responds to deformations via inhomogeneous and an-isotropic rearrangements and stress-response. An initially isotropic contact network becomes an-isotropic before the structure of the network reaches its limit of stability, i.e., the yield stress. Before the peak, one has softening, and beyond weakening is obtained [2-5], which is typical for over-consolidated powders. Our work complements recent studies on shear band formation in frictional-cohesive granular media [4-8], for micro- and macro-modeling [9,10], and in various systems [11-14] for different materials.

Besides spheres, non-spherical particles like polygons can also be used [10], or rougness can be mimicked by additional torques [15]. The recently developed micro-macro transition procedures [6-13] aim at a better understand of the macroscopic powder flow behavior on microscopic foundations. Besides the experimental verification of the simulation results [14], the formulation of constitutive relations in the framework of continuum theory is the great challenge. One promising material model for sand is the hypoplastic theory [16-20], for which the material parameters can be determined experimentally, or from DEM simulations, as shown in this study.

## 2 Model

### 2.1 Simulation Details

The elementary units of granular materials are ”mesoscopic” grains that locally, at the contact point, deform under stress. Since the realistic modeling of the deformations of the particles is much too complicated, the interaction force is related to the overlap $\Delta$ of two particles, see Fig. 1. Two particles interact only if they are in contact, and the force between these two particles is decomposed into a normal and a tangential part. For the sake of simplicity, we restrict ourselves to spherical particles here. The normal force is, in the simplest case, a linear spring that takes care of repulsion, and a linear dashpot that accounts for dissipation during contact. The tangential force involves dissipation due to Coulomb friction, but also some tangential elasticity that allows for stick-slip behavior on the contact level [4,9,10,13,14].

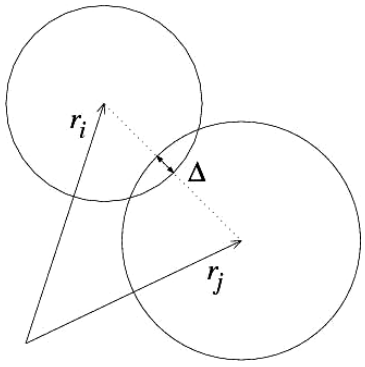


Figure 1: Two particle contact with overlap $\Delta$.

If all forces acting on a selected spherical particle (either from other particles, from boundaries or from external forces) are known, the problem is reduced to the integration of Newton's equations of motion for the translational and rotational degrees of freedom:

$$m_i \frac{\mathrm{d}^2}{\mathrm{d}t^2}\mathbf{r}_i = \mathbf{f}_i + m_i\mathbf{g} \quad \text{and} \quad I_i \frac{\mathrm{d}}{\mathrm{d}t}\boldsymbol{\omega}_i = \mathbf{t}_i \ , \qquad (1)$$

with the gravitational acceleration $\mathbf{g}$, mass $m_i$ of the particle, its position $\mathbf{r}_i$, the total force $\mathbf{f}_i = \sum_c \mathbf{f}_i^c$, acting on it due to contacts with other particles or

with the walls, its moment of inertia $I_i$, its angular velocity $\boldsymbol{\omega}_i$, and the total torque $\mathbf{t}_i = \sum_c \mathbf{l}_i^c \times \mathbf{f}_i^c$, with the center-contact "branch" vector $\mathbf{l}_i^c$.

### 2.2 Model System

The simulations with the discrete element model [4-10] use a two-dimensional bi-axial box, see Fig. 2, where the left and bottom walls are fixed. Stress- or strain-controlled deformation is applied to the side- and top-walls, respectively. In a typical simulation, the top wall is slowly shifted downwards, while the right wall moves, controlled by a constant stress $p_x$, responding on the forces exerted on it by the material in the box. The motion of the top-wall follows a cosine function, in order to allow for a smooth start-up and finish of the motion so that shocks and inertia effects are reduced, however, the shape of the function is arbitrary as long as it is smooth.

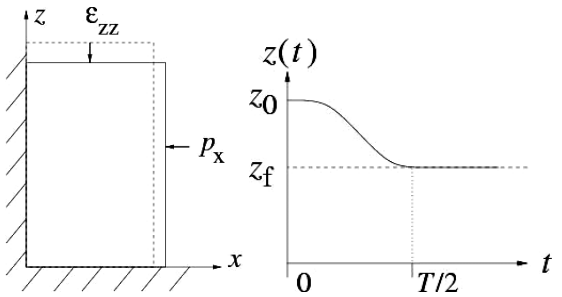


Figure 2: (Left) Schematic drawing of the model system. (Right) Position of the top-wall as function of time for the strain-controlled situation.

### 2.3 Initial conditions

Initially, the particles are randomly distributed in a huge box, with rather low overall density. Then the box is compressed by defining an external pressure *p*, in order to achieve an isotropic initial condition. Starting from this relaxed, isotropic configuration, the strain $\varepsilon_{zz}$ is applied to the top wall and the response of the system is examined.

## 3 Results

The system examined in the following contains *N*=1950 particles with radii randomly drawn from a homogeneous distribution with minimum 0.5 mm and maximum 1.5 mm. The friction coefficient used in the two-dimensional simulations is $\mu$=0.5.

### 3.1 Stress-strain measurement

In Fig. 3 (top), the volume change of a typical simulation shows first compression, then dilatancy, and eventually a very weak change at very large deformations, up to 20 per-cent. At the same time, the stress response, in Fig. 3 (bottom) (where the indices xx and zz denote horizontal and vertical stresses, respectively), shows elastic, softening, and critical state flow behavior. First, the vertical stress increases linearly; then the slope gradually decreases (softening), until the stress reaches its maximum (peak yield stress). After the peak, further softening/weakening behavior (with negative slope) is followed by a constant, strongly fluctuating stress for larger deformations.

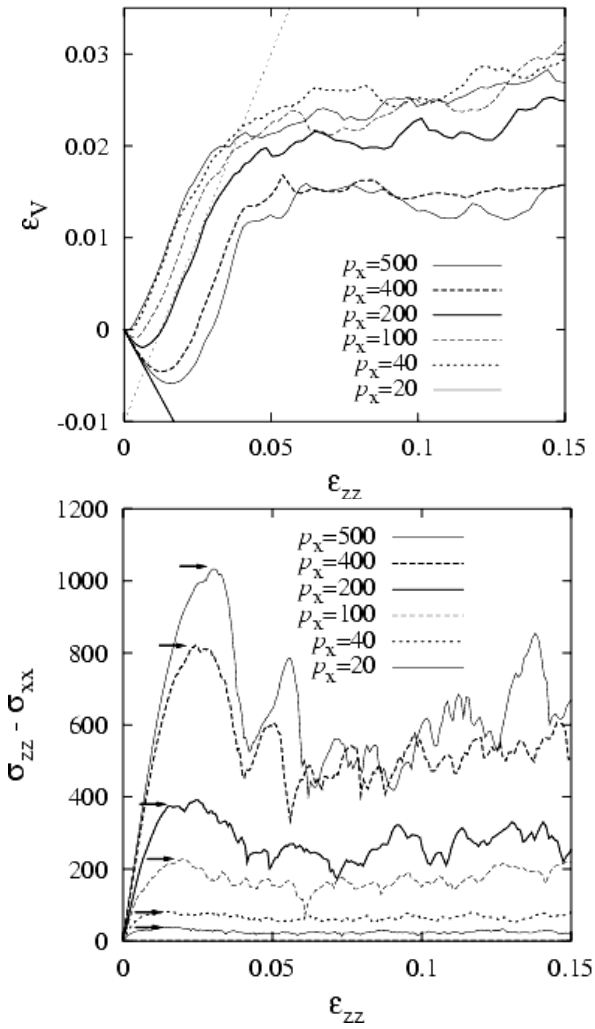


Figure 3: Volumetric strain (top) and stresses (bottom) during large deformations, both plotted against vertical strain, for different side pressure, as indicated in the inset. The peak yield stress is marked by arrows.

### 3.2 Macroscopic material parameters

From the simulation data presented in Fig.3, it is possible to obtain the following material parameters, as based on an isotropy assumption:

(i) The initial slope (-0.59) of the volumetric strain allows to determine the Poisson ratio.

(ii) The slope of the volumetric strain in the dilatancy regime (0.80) is related to the dilatancy angle.

(iii) The initial slope of the stress is related to the bulk modulus (data not shown here).
(iv) The peak (yield) stress is related to the flow function of the material, as discussed in detail in the next subsection.

### 3.3 Peak flow function

It is possible to examine the flow behavior of the system by plotting Mohr-circles for the maximum stress (right-most point on the circle) for different confining pressures (left-most point), see Fig. 4. The eigen-directions of the system are parallel to the walls, because there is no friction active between particles and walls, so that the left- and right-most points on the circles are indeed corresponding to the wall stresses; note that in an arbitrary geometry, it is not necessarily that simple. The tangent to the circles (slope 0.588) can be seen as the flow function for peak stress. It is linear for the examined parameters, with its slope only slightly larger than expected from the microscopic friction at the contacts alone. Since we have not used cohesive forces, the macroscopic cohesion $c$ is non-existent, i.e., the flow function hits the origin.

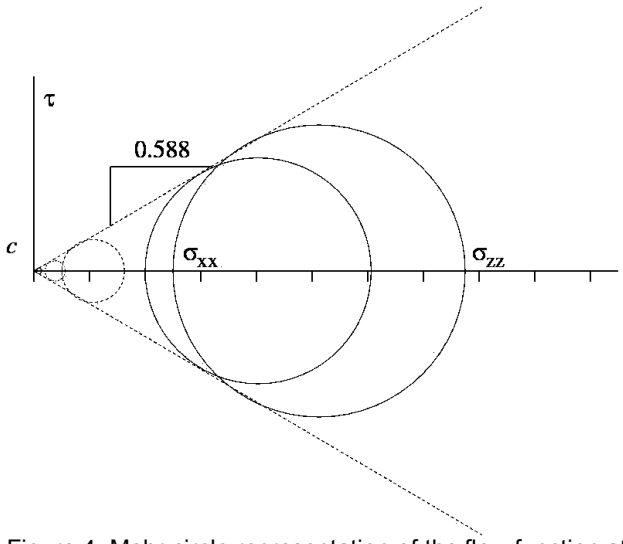


Figure 4: Mohr circle representation of the flow function at peak stress, see the arrows in Fig. 3 (bottom).

### 3.4 Some material parameters for Hypoplasticity

Some of the material parameters involved in a hypoplastic material theory [16-20] can also be extracted from the simulation data. An essential ingredient of the theory is the functional behavior of the pore number:

$$e^h = e_0^h \exp\left(-\left[p/h_s\right]^n\right) , \qquad (2)$$

as a function of the pressure. The empirical model parameters for this function (based on experimental findings) involve the pore number at vanishing stress, $e_0^h$, the so-called granular hardness, $h_s$, and an empirical power $n$.

The function in Eq. (2) is astonishingly close to the fit-function for the initial and the critical state pore-number envelope, see Fig. 5:

$$e\left(e_0, n\right) = e_0 - \left[p/h_s\right]^n , \qquad (3)$$

where the parameters $e_0$ and $n$ can be read off from the inset, and the granular hardness was set equal to the spring stiffness $h_s = 10^5$ in the DEM contact model. Eqs. (2) and (3) can be related to each other via a series expansion in the small variable $p/h_s$.

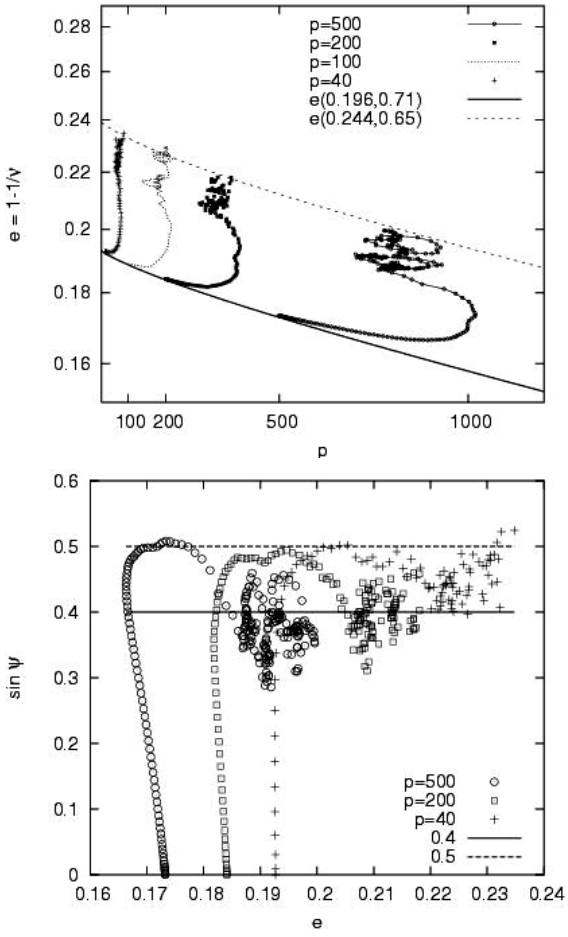


Figure 5: Pore number plotted against side stress (top), and deviatoric stress ratio plotted against pore number (bottom) – for different confining pressures.

The representation of the deviatoric stress ratio

$$\sin\psi = \frac{\sigma_{zz} - \sigma_{xx}}{\sigma_{zz} + \sigma_{xx}} , \qquad (4)$$

in Fig. 5 (bottom) is another way to extract the macroscopic friction angle. For peak stress, the simulations are almost in agreement with the microscopic friction coefficient $\mu$=0.5, whereas for the peak stress (besides strong scatter due to fluctuations), the macroscopic friction angle decreases with increasing pressure. For the largest

pressure used here, the friction coefficient is smaller than $\mu$=0.4.

## 4 Summary and Conclusions

In summary, a set of DEM simulations was presented, and several macroscopic material parameters like, e.g., the friction angle were extracted from the data. Also the behavior of density (pore-number) and friction angle as function of the confining pressure were discussed and related to a hypoplastic material law [16-20].
The present results are a first step of a micro modeling approach for cohesive frictional powders. Further material parameters have to be identified, and also the effect of cohesion has to be examined more closely, not only for frictionless [11-13], but also for frictional materials.
Also the role of particle rotations is an open issue, as related to micro-polar constitutive models. In both simulation and experiment, rotations are active in the shear band – like in micro-polar hypoplastic material models, where the rotational degree of freedom is activated in the shear band too. The corresponding parameter identification and the micro-macro-transition is another task for the future, like the implementation and simulation in three-dimensional systems.

**ACKNOWLEDGEMENTS**

This work was funded by the Deutsche Forschungsgemeinschaft (DFG) in the framework of the research-group: “Verhalten Granularer Medien”; we acknowledge helpful and inspiring discussions with H.-J. Butt, M. Kappl, M.-K. Müller, K. Nübel, R. Pitchumani, J. Tejchman, J. Tomas, and R. Tykhoniuk.

## REFERENCES

[1] H. J. Herrmann, J.-P. Hovi, and S.Luding, eds., *Physics of dry granular media*, NATO ASI Series E 350, Kluwer Academic Publishers, Dordrecht, 1998.
[2] P. A. Vermeer, S. Diebels, W. Ehlers, H. J. Herrmann, S. Luding, and E. Ramm, eds., *Continuous and Discontinuous Modelling of Cohesive Frictional Materials*, Lecture Notes in Physics 568, Springer, Berlin, 2001.
[3] Y. Kishino, ed., *Powders & Grains 2001*, Balkema, Rotterdam, 2001.
[4] C. Thornton and S. J. Antony, Quasi-static deformation of a soft particle system, Powder Technology 109(1-3), 179—191, 2000.
[5] G. A. D'Addetta, F. Kun, E. Ramm, *On the application of a discrete model to the fracture process of cohesive granular materials*, Granular Matter 4 (2), 77-90 2002.
[6] M. Oda and K. Iwashita, *Study on couple stress and shear band development in granular media based on numerical simulation analyses*, Int. J. of Enginering Science 38, 1713-1740, 2000.
[7] N. P. Kruyt and L. Rothenburg, *Statistics of the elastic behavior of granular materials*. Int. J. of Solids and Structures 38, 4879—4899, 2001.
[8] S. Luding, M. Lätzel, W. Volk, S. Diebels, and H. J. Herrmann, *From discrete element simulations to a continuum model*, Comp. Meth. Appl. Mech. Engng. 191, 21-28, 2001.
[9] J. Tomas, *Assessment of mechanical properties of cohesive particulate solids – part 1: particle contact constitutive model*, Particulate Sci. Technol. 19, 95-110, 2001.
[10] J. Tomas, *Assessment of mechanical properties of cohesive particulate solids – part 2: powder flow criteria*, Particulate Sci. Technol. 19, 111-129, 2001.
[11] R. Tykhoniuk, and J. Tomas, *Simulation der Scherdynamik von kohäsiven Pulvern*, Chem. Ing. Techn. 75, (in press) 2003.
[12] S. Luding and H. J. Herrmann, *Micro-Macro Transition for Cohesive Granular Media* ,in: Zur Beschreibung komplexen Materialverhaltens, Institut für Mechanik, S. Diebels (Ed.), Stuttgart, 121--134, 2001.
[13] S. Luding, R. Tykhoniuk, and Jürgen Tomas, *Anisotropic material behavior in dense, cohesive powders*, Chem. Eng. Tech., in press, 2003.
[14] M. Lätzel, S. Luding, H. J. Herrmann, D. W. Howell, and R. P. Behringer, *Comparing Simulation and Experiment of a 2D Granular Couette Shear Device,* Eur. Phys. J. E 11, 325-333, 2003.
[15] M. Oda, *Micro-fabric and couple stress in shear bands of granular materials*, in: Powders and Grains, C. Thornton, ed., Rotterdam, Balkema, 161-167, 1993.
[16] J. Tejchman and W. Wu, *Numerical study on patterning of shear bands in a Cosserat continuum*, Acta Mechanica 99: 61-74,1993.
[17] E. Bauer and W. Huang, *Numerical study of polar effects in shear zones*, in: Numerical Models in Geomechanics, G.N. Pande, S. Pietruszczak, H. F. Schweiger, eds., Balkema, 133-141, 1999.
[18] E. Bauer, *Calibration of a comprehensive hypoplastic model for granular materials,* Soils and Foundations 36, 13-26, 1996.
[19] J. Tejchman, *Patterns of shear zones in granular materials within a polar hypoplastic continuum*, Acta Mechanica 155, 71-95, 2002.
[20] K. Nübel, *Experimental and Numerical Investigation of shear localization in granular material*, PhD thesis, Karlsruhe, 2002.